STRONG MOTION MOLECULAR-ELECTRONIC ACCELEROMETER

Ph.D. student Ivan Egorov[1]

Academician Alexander Bugaev[2]

Graduate student Dmitry Chikishev[3]

[1] Moscow Institute of Physics and Technology, **Russia**
[2] Moscow Institute of Physics and Technology, **Russia**
3 Moscow Institute of Physics and Technology, **Russia**

ABSTRACT

During an earthquake, a strong ground motion arises not only in the focus, but it also extends over long distances. Strong motion data have to be used in the Earthquake Early Warning (EEW) for a quick response of rescue services and monitoring of building structures. As the speed of the waves propagation in the ground is sufficiently high (about a few km/s), the warning time must be little, but sufficient to alert the people. Structural and earthquake engineers can use strong motion data to verify or improve design codes. Also, since seismic sensors are becoming more common, it is now possible to correlate the expected damage with instrument readings.

Molecular-electronic transfer (MET) accelerometers are increasingly competing with MEMS accelerometers to measure strong motion. Technology allows designing an accelerometer with a wide frequency range (0.05 to 150 Hz) and a maximum recorded signal +- 3g. At the same time, it has a low noise level of 1 μg at 10 Hz, reaching dynamic range of 130 dB.

This work studies the effect of large input signals on the parameters of a MET converter. A mathematical model including nonlinear parts for theoretical studies of the dependence of the output signal was produced. Also, experimental studies were conducted, including comparisons to similar MEMS accelerometers. Comparative data were obtained by several methods:

- on a shake table that can imitate an earthquake
- on a shake table that can produce strong sinusoidal vibration
- by using self-calibration.

As a result, the data shown in the experimental part make it possible to use MET accelerometers in many areas where there is a strong motion.

Keywords: electrochemical devices, molecular-electronic transfer, nonlinear effects

INTRODUCTION

The sensory element based on a molecular-electronic transfer consists of a four-electrode system placed in an electrolyte. The principle of the operation is based on the fact that during the electrolyte movement through the electrode cell, the concentration of the electrolyte components near the electrodes changes, thereby changing the electric current flowing between the pairs of electrodes (Fig. 1). Such electrochemical sensors are

used to detect linear and angular movements in a wide frequency range from 120 s up to 500 Hz and in a dynamic range of up to 140 dB.

In earlier works, the operation principle of the MET sensor for various geometric models of the electrode system [1], [2], [3] was described. Particular attention was paid to the study of the MET sensor self-noise and the methods for reducing it [4], [5], [6]. Recent works describe the processes of the signal currents flow in the MET sensor with more accurate boundary conditions for the equation of convective diffusion [7]. The flow speed was assumed to be small.

However, MET sensors now successfully occupy the field of large signals measuring [8]. Therefore, it has become relevant to understand the processes taking place in the MET sensor at large signals [9], [10], [11], [12].

This article discusses the model proposed in [12], [13]. The main goal is to study the effect of nonlinear additions in the convective diffusion equation. The experimental part involves building the dependence of the constant component of the signal current on the amplitude of the input signal. The achievement of the maximum measured MET signal of the MTSS1031A accelerometer and the comparative analysis of the record of simulated earthquakes on a mechanical stand together with MEMS MS1000 by Colibrys was also studied.

THEORY

In [11], the model of the electric current flow in the four electrode system in an aqueous solution of $KI+I_2$ electrolyte is described in detail. It takes into account the conditions and mechanisms of the of electric current flow through the double electric layer and the electrodes surface for each of the components of the electrolyte solution.

As a result, we use the final system of equations:

$$\frac{\partial C}{\partial t} = D\Delta C - \overline{V}\nabla C \qquad (1)$$

where C is the I_3^- ions concentration, D is the I_3^- ions diffusion coefficient, $\overline{V}$ is the flow speed of the electrolyte solution through the electrode cell.

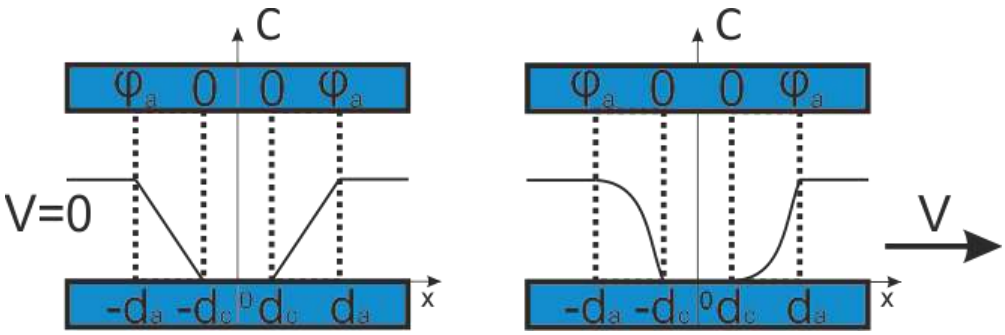

Fig. 1. Layout of anodes and cathodes in the converting cell and I_3^- concentration distribution in the motion absence (left) and during the electrolyte flow when a constant potential φ_a is applied to the anodes (right).

In this work we consider a one-dimensional model of a transforming cell, the layout of which is shown in Fig. 1. The electrodes are endless plates, which are permeable to the electrolyte solution. Potential φ_a is applied on the anodes relative to the cathodes, the potential of which is 0.

Since the stationary case, when the electrolyte solution does not flow through the electrode system, is considered in the same paper [10], attention should be paid to the dynamic case, when the electrolyte flows at a speed varying according to the harmonic law $V = V_0 sin\omega t$.

We find a solution to the equations (1) in the form of expansions in powers of *V* to order 2:

$$C = C^{(0)} + C^{(1)} + C^{(2)} \qquad (2)$$

where $C^{(0)} \sim V^0, C^{(1)} \sim V^1, C^{(2)} \sim V^2$. Then the equation (1) is converted into a system of equations:

$$\begin{cases} \frac{\partial^2 C^{(0)}}{\partial x^2} = 0 \\ \frac{\partial C^{(1)}}{\partial t} = D\frac{\partial^2 C^{(1)}}{\partial x^2} - V_0 sin\omega t \frac{\partial C^{(0)}}{\partial x} \\ \frac{\partial C^{(2)}}{\partial t} = D\frac{\partial^2 C^{(2)}}{\partial x^2} - V_0 sin\omega t \frac{\partial C^{(1)}}{\partial x} \end{cases} \qquad (3)$$

The solutions of the first equation of the system (3) in the region determining the cathode currents $-d_a < x < d_c$, $d_c < x < d_a$ looks like $C^{(0)} = Ax + B$. Then for $C^{(1)}$ the equation will transform in the following way:

$$\frac{\partial C^{(1)}}{\partial t} = D\frac{\partial^2 C^{(1)}}{\partial x^2} - V_0 A sin\omega t \qquad (4)$$

The solution of such an equation is $C^{(1)} = C_1(x)\, sin(\omega t + \gamma)$. To search for the additive $C^{(2)}$ substitute the dependence $C^{(1)}$ into the third equation of system (3) and obtain the following expression:

$$\frac{\partial C^{(2)}}{\partial t} = D\frac{\partial^2 C^{(2)}}{\partial x^2} - \frac{V_0}{2}\frac{\partial C_1(x)}{\partial x}(cos\gamma - cos(2\omega t + \gamma)) \qquad (5)$$

The solution of this equation is the following relationship:

$$C^{(2)} = F(x)\, sin\, 2\omega t + G(x) cos 2\omega t + Q(x) \qquad (6)$$

The total electrical current flowing through the anode-cathode pair is determined by ∇C. ∇C. Consequently, taking into account the nonlinear terms of expansion in powers of *V*, a constant current additive $q \sim {V_0}^2$ appears. The total electric current has the following relationship:

$$I(V_0, t) = I_0 + I_1(V_0, \omega t) + I_2\left({V_0}^2, 2\omega t\right) + q(V_0^2) \qquad (7)$$

Here, I_0 is the background current, which is determined by the stationary case, I_1, I_2 are the signal currents that occur when the electrolyte moves through the electrode structure, $q({V_0}^2)$ is the constant current component depending on the electrolyte speed.

EXPERIMENT AND RESULTS

The experiment was conducted on a MET sensitive element of the MTSS 1031A accelerometer manufactured by R-Sensors, the layout of which is shown in Fig. 2. The electrical signal current arising in the electrode system 1 is converted in the electronic board 6 and fed to the inductance 5. By interacting with the permanent magnet 4, it creates

a counter-force to the external acceleration, reducing the speed of the electrolyte flow through the electrode system. Membranes 3 are the elastic element of this system.

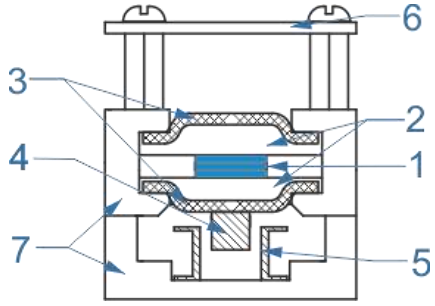

Fig. 2. The MET layout of the MTSS 1031 A accelerometer with negative feedback, where 1 - electrode system enclosed in a ceramic case, 2 - electrolyte solution, 3 - membrane, 4 - permanent magnet, 5 - inductor, 6 - electronic board, 7 - outer case.

The circuit diagram of the electronics is shown in Fig. 3. The electric current arising in the sensing element is converted to voltage in the first cascade of the electronics W_1. The W_2 cascade is used for amplitude-frequency correction of the signal. β forms a signal for the negative feedback block. The W_{filter} cascade forms the output frequency range of the accelerometer MET.

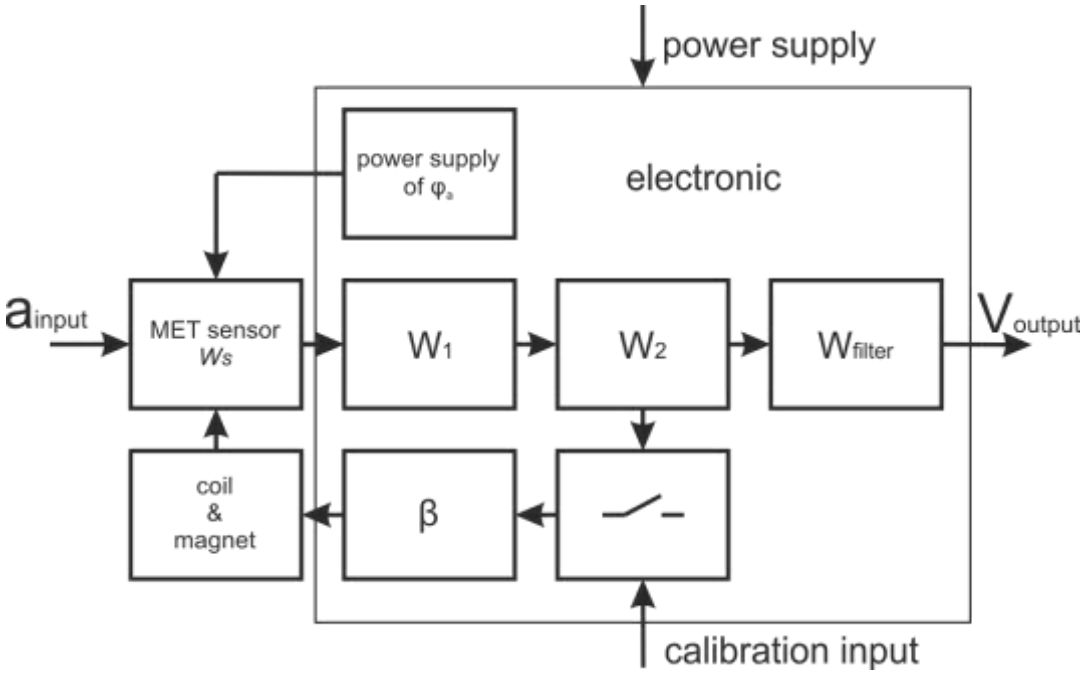

Fig. 3. Schematic diagram of the MET accelerometer electronics.

The W_1, W_2 cascades also contain thermal compensating part, which allows the use the accelerometers in a wide temperature range. In this case, the transfer function of the accelerometer is determined by the following expression:

$$W_{acc} = \frac{W_{sensor} W_1 W_2}{1 + W_{sensor} W_1 W_2 \beta} W_{filter} \qquad (8)$$

You can notice that at $W_{sensor}W_1W_2\beta \gg 1$ the accelerometer properties are determined by the values of β.

In the course of the experiment, a harmonic signal from a voltage generator was applied to the calibration input of the electronic circuit, which was converted into a current in the coil of the feedback circuit and by interacting with a magnet on the membrane caused the electrolyte to move through the electrode assembly. To eliminate the influence of the establishment process, for each amplitude, the recording was more than 100 periods. Further, the average value was calculated for a plot of a multiple of the period. I_0 was determined at the recording site without a harmonic signal. As a result, the additive value $q(V_0^2) = \langle I \rangle - I_0$ was calculated.

Fig. 4 shows the graphs of the dependences of the constant components of the cathode currents on the magnitude of the input signal for the frequency of 10 Hz for two cases. The black graph corresponds to the q dependence for the MET accelerometer sensitive element, which is not covered by feedback. The grey one corresponds to the q dependence for sensitive element with closed feedback. For each case, an approximating power function $y=x^n$ was constructed. The exponents were n_1=1.86 and n_2=2.11, which turned out to differ from the theoretically assumed n_0=2 by less than 10%. This suggests that the theoretical model was constructed adequately, and the errors are related to the one-dimensionality of the model and the experimental errors. The advantage of using deep negative feedback was also experimentally shown, since the manifestation of the influence of strong signals for the MET accelerometer sensitive element with a closed feedback turns out to be in the range of amplitudes 20 times larger than for the sensitive element not covered by feedback, which corresponds to the parameter $K\beta$ for the selected accelerometer sample.

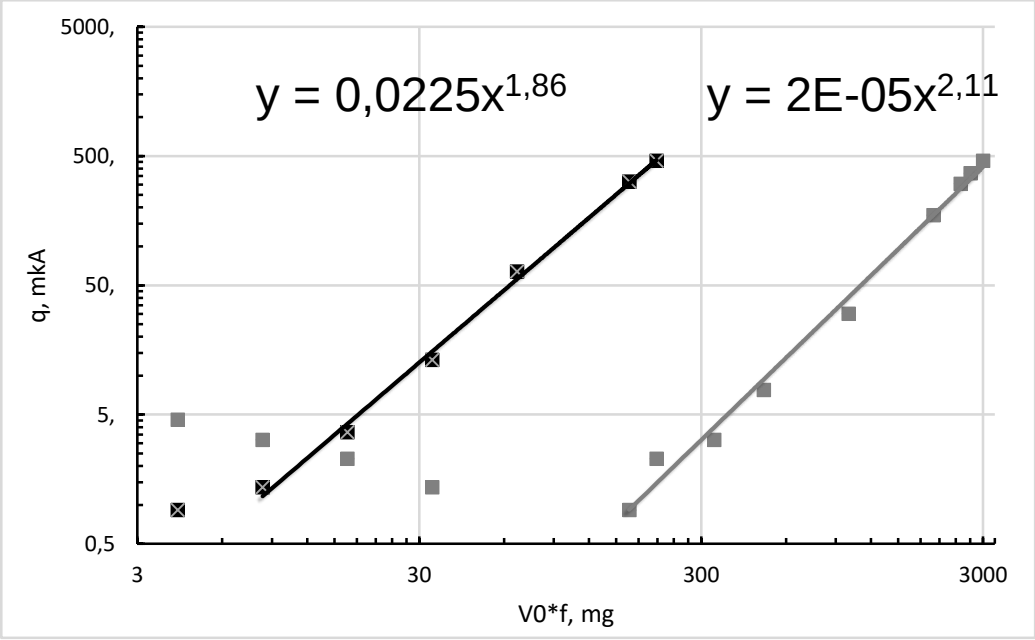

Fig. 4. The dependence of the constant component on the magnitude of the input signal. Black is the MET accelerometer sensitive element, not covered by feedback, grey is the sensitive element with closed feedback.

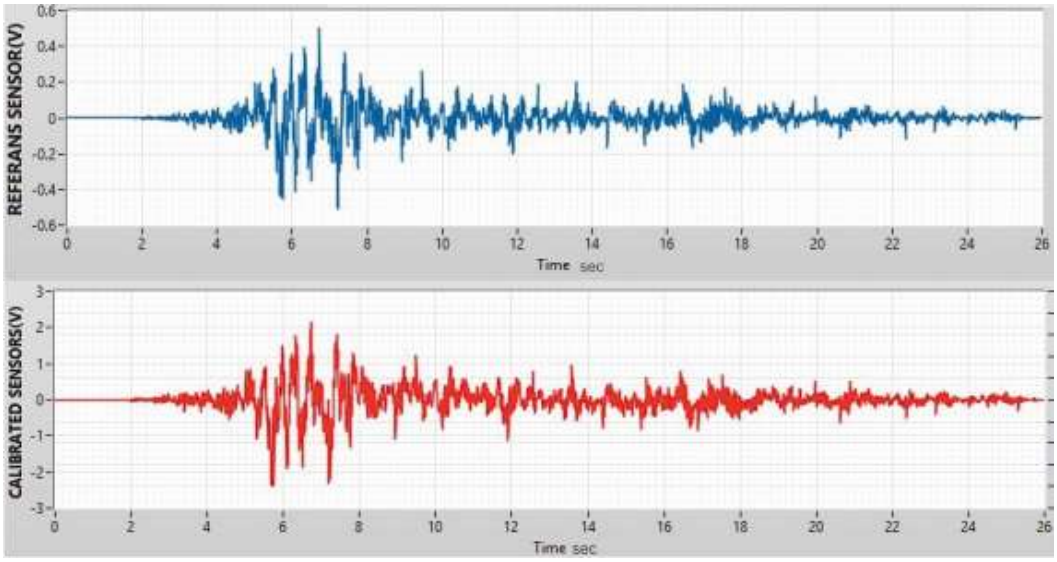

Fig. 5. Data of earthquake simulation on a mechanical table: blue – for MS1000 with a sensitivity of 0.5 V/g; red – MTSS1031A with a sensitivity of 2.4 V/g.

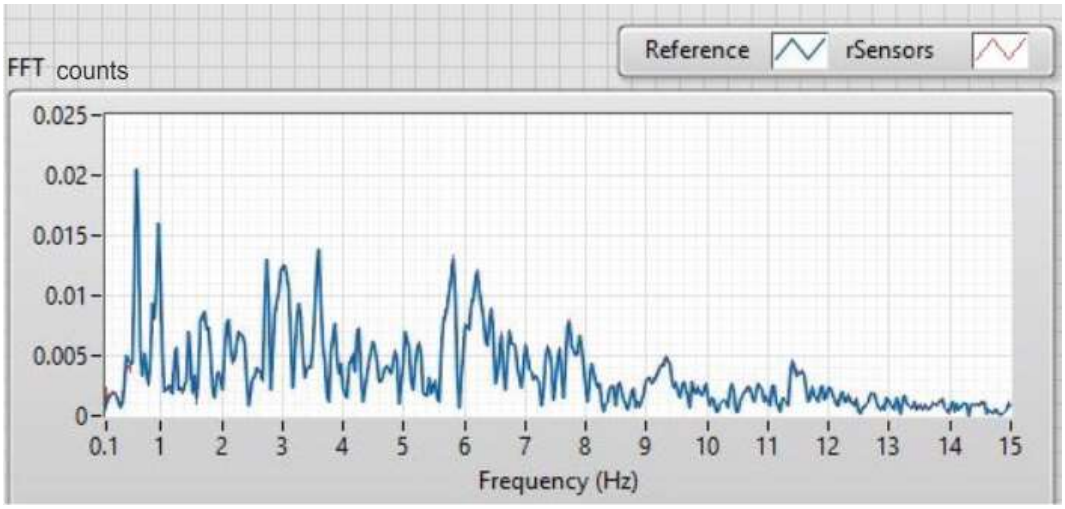

Fig. 6. Spectra of the earthquake simulation records: blue - MS1000; red – MTSS1031A.

CONCLUSION

The obtained results show that the constructed mathematical model adequately describes the experimental data. In particular, it was revealed that when a harmonic signal is applied to the molecular-electronic cell of the MET converter, the signal electric current between the anode-cathode pair has a constant component, which depends on the flow speed of the electrolyte solution through the electrode system and looks the following way:

$$q \sim {V_0}^2 \qquad (9)$$

The differences between the experimental and theoretical data are associated with simplifications made in the mathematical model and statistical errors in the experimental values measurement.

Also, the data obtained show that when developing an electronic circuit, it is essential to choose electronic components carefully. With large disturbing input effects, the signal electric current transformed into voltage in the first cascade W_1 can switch the operational amplifier to saturation mode. This will serve as a restriction for the detection of maximum signals and adversely affect the accelerometer operation as a whole.

The experimentally obtained maximum signal of ± 3 g with self-noise level of 1 μg allows achieving a dynamic range of 130 dB. The coefficient of nonlinear distortion CND corresponds to the level of <0.5%. These parameters, together with a comparative analysis of earthquake simulated recordings on a mechanical stand, allow competing with MEMS accelerometers designed to detect strong disturbances in such areas as earthquake warning systems and monitoring structures and buildings.

ACKNOWLEDGEMENTS

The research was supported by Russian foundation of basic research Project 17-20-02183 ofi-m-rzd.

Thanks to Eren Aydın from Teknik Destek Grubu Ltd for providing experimental data.

REFERENCES

[1] Sun Z. et al., "A MEMS Based Electrochemical Seismometer with Low Cost and Wide Working Bandwidth," Procedia Eng., vol. 168, pp. 806–809, 2016.

[2] Deng T., Chen D., Chen J., Sun Z., Li G., Wang J., Microelectromechanical Systems-Based Electrochemical Seismic Sensors with Insulating Spacers Integrated Electrodes for Planetary Exploration, IEEE Sens. J., vol. 16, no. 3, pp. 650–653, 2016.

[3] Bugaev A. S. et al., Measuring Devices Based on Molecular-Electronic Transducers, J. Commun. Technol. Electron., vol. 63, no. 12, pp. 1339–1351, 2018.

[4] Zaitsev D. L., Avdyukhina S. Y., Ryzhkov M. A., Evseev I., Egorov E. V., Agafonov V. M., Frequency response and self-noise of the MET hydrophone, J. Sens. Sens. Syst., 7, 443-452, https://doi.org/10.5194/jsss-7-443-2018, 2018.

[5] Zaitsev D. L., Agafonov V.M., Evseev I.A., Study of Systems Error Compensation Methods Based on Molecular-Electronic Transducers of Motion Parameters, Journal of Sensors, vol. 2018, Article ID 6261384, 9 pages, 2018. https://doi.org/10.1155/2018/6261384.

[6] Agafonov V.M., Modeling the Convective Noise in an Electrochemical Motion Transducer, Int. J. Electrochem. Sci., vol. 13, p. 11442, 2018.

[7] Agafonov V.M., Egorov E.V., Influence of the electrical field on the vibrating signal conversion in electrochemical (MET) motion sensor, Int. J. Electrochem. Sci., vol. 11, no. 3, pp. 2205–2218, 2016.

[8] Zaitsev D.L., Egorov E.V., Shabalina A.S., High resolution miniature MET sensors for healthcare and sport applications, 2018 12th International Conference on Sensing Technology (ICST), Limerick, 2018, pp. 287-292.doi: 10.1109/ICSensT.2018.8603579

[9] Zhou Q., Wang C., Chen Y., Chen S., Lin J., Dynamic response analysis of microflow electrochemical sensors with two types of elastic membrane, Sensors (Switzerland), vol. 16, no. 5, 2016.

[10] Wang J., Zhang Z., Li G., Chen D., Chen J., Electrochemical vibration sensor with force balance feedback system, in 2015 IEEE SENSORS - Proceedings, 2015.

[11] Egorov I. V, Shabalina A. S., Agafonov V. M., Design and Self-Noise of MET Closed-Loop Seismic Accelerometers, IEEE Sens. J., vol. 17, no. 7, pp. 2008–2014, 2017.

[12] Agafonov V.M., Egorov E.V., Electrochemical accelerometer with DC response, experimental and theoretical study, J. Electroanal. Chem., vol. 761, 2016.

[13] Agafonov V. M., Egorov E. V., Bugaev A. S., Application of the convective diffusion equation with potential-dependent boundary conditions to the charge transfer problem in four-electrode electrochemical cell on the condition of small hydrodynamic velocity, Int. J. Electrochem. Sci., vol. 11, no. 2, 2016.